Flavour Structure of the Baryon Octet

G. S. Bali, S. Collins for the RQCD Collaboration

published in

NIC Symposium 2020
M. Müller, K. Binder, A. Trautmann (Editors)

Forschungszentrum Jülich GmbH,
John von Neumann Institute for Computing (NIC),
Schriften des Forschungszentrums Jülich, NIC Series, Vol. 50,
ISBN 978-3-95806-443-0, pp. 175.
http://hdl.handle.net/2128/24435

© 2020 by Forschungszentrum Jülich
Permission to make digital or hard copies of portions of this work for personal or classroom use is granted provided that the copies are not made or distributed for profit or commercial advantage and that copies bear this notice and the full citation on the first page. To copy otherwise requires prior specific permission by the publisher mentioned above.

Flavour Structure of the Baryon Octet

Gunnar S. Bali and Sara Collins
for the RQCD Collaboration

Institut für Theoretische Physik, Universität Regensburg, 93040 Regensburg, Germany
E-mail: {gunnar.bali, sara.collins}@ur.de

We investigate aspects of the structure of different baryons via simulations of quantum chromodynamics in lattice regularisation (Lattice QCD). In particular, we study the mass spectrum, (generalised) isovector charges as well as moments of light cone distribution amplitudes. The charges correspond to moments of parton distribution functions (PDFs). Almost all visible matter in the universe consists of nucleons (*i. e.* protons and neutrons), which are also the prime probes for new physics, be it in accelerator experiments or dark matter and neutrino detectors. The results will increase the precision of the relation between experimental cross sections and decay rates and the underlying fundamental theory, which describes interactions on the quarks and gluon level rather than interactions with the nucleons (which are composed of quarks and gluons). By extending the study to so-called hyperons that contain strange quarks, in addition to the up and down quarks of the nucleon, at many different quark mass combinations, the validity range of chiral perturbation theory (ChPT) and quark flavour symmetry relations can be checked and low energy constants predicted.
The simulations are carried out in $N_f = 2 + 1$ QCD, neglecting the mass difference between up and down quarks and the electric charges of the quarks. We employ Coordinated Lattice Simulations (CLS) gauge ensembles. These were generated in a Markov chain using the hybrid Monte Carlo (HMC) algorithm with open boundary conditions in time, on several European supercomputers including JUWELS and JUQUEEN. The Wilson fermion discretisation is used, with non-perturbative removal of lattice spacing effects that are proportional to the lattice constant (order a improvement). The main computational task in the analysis that is carried out on the Xeon-Phi Booster module of JURECA of these gauge ensembles with volumes ranging from $64 \cdot 32^3$ up to $192 \cdot 96^3$ points, encompassing 1000–2000 configurations each, is the multiple solution of sparse large linear systems with a dimension of up to $(2 \cdot 10^9)^2$ complex variables. This is achieved by an adaptive algebraic multigrid algorithm. A novel stochastic method allows us to obtain results for four different baryons and many momentum combinations with little computational overhead, relative to just computing the structure of the nucleon at a few momenta.

1 Introduction

With the discovery of the Higgs boson at the LHC at CERN in 2012 the existence of the last missing particle predicted by the Standard Model was confirmed. Since then (and also before then) the Standard Model, which is the accepted theory of elementary particles and their interactions, successfully passed an impressive number of precision tests, *e. g.* at the LHC, B-factories and low energy β decay experiments. At present only a few observables show tensions with respect to experiment on the level of three standard deviations. Yet we know that the Standard Model in its present form is incomplete. For instance, from cosmological observations one can infer the existence of the so-called Dark Matter that at present has only been detected via its gravitational interaction. This matter is distributed differently in galaxies than one would expect from the particles that are included in the Standard Model and interactions between this matter and Standard Model matter must be very weak. Another issue is the abundance of matter over antimatter in the early universe,

which requires a significant breaking of the so-called CP-symmetry and a first order phase transition, which the Standard Model fails to explain. Finally, there are unresolved questions in the neutrino sector and the puzzle why differences between masses of elementary particles are so large, ranging from the top quark ($m_t \approx 1.7 \cdot 10^{11}$ eV) down to the lightest neutrino ($m_{\nu_1} < 0.9 \cdot 10^{-1}$ eV[1]).

The Standard Model unifies the electromagnetic and weak interactions and contains the theory of strong interactions (QCD) that bind quarks and gluons into hadrons (*e. g.* protons and pions). In order to discover deviations between experiment and Standard Model predictions, a new level of precision is required, and once deviations are seen, theory input will be needed to relate experimental (differential) cross sections and life times to the couplings between fundamental particles. The accuracy of this is often limited by theoretical rather than experimental uncertainties and, in particular, by hadronic uncertainties: almost all visible matter of the universe consists of nucleons, which are also the prime probe for new physics, be it in collider experiments, long baseline neutrino oscillation experiments or direct dark matter detection. These are made up of strongly interacting quarks and gluons, whose interactions are often elusive to analytical approaches and hence many aspects of hadron structure and in particular of nucleon structure are not very well determined. Fits to experimental data, sometimes employing flavour symmetry arguments and/or chiral perturbation theory (ChPT), still dominate our knowledge. As pointed out above, clarifying the structure of nucleons in terms of their quark and gluon components in a rigorous way is of great importance. In principle this can be achieved by *ab initio* Lattice QCD simulations of the underlying theory.

In the last decade Lattice QCD simulations have reached the quark masses, lattice volumes and spacings and statistical precision required to make an impact in this field. Since then discrepancies with phenomenological estimates have shown up. For instance the nucleon σ term, which determines the strength of the coupling of the proton to hypothetical new matter either via Higgs exchange or directly, when extracted from fits to pion nucleon scattering[2, 3] comes out by a factor of almost two larger than when determined directly in lattice simulations close to the physical quark mass point.[4–7] Clearly, the systematics need to be understood better, also on the phenomenological side.

Here, we study several observables related to baryon structure to shed light on these questions. Below we list some of the highlights of our present and ongoing large scale simulation programme.

- We achieve an excellent coverage of the plane spanned by the strange quark mass m_s and the light quark mass $m_\ell = m_u = m_d$, enabling us not only to extrapolate or interpolate to the physical point but also to verify effective field theory predictions and in particular covariant baryon chiral perturbation theory (BChPT).
- We cover a large bracket of lattice spacings reaching down to $a < 0.04$ fm $= 4 \cdot 10^{-17}$ m. Usually, the hybrid Monte Carlo (HMC) and other updating algorithms based on local changes will slow down exponentially with the inverse lattice spacing beyond a value $a \lesssim 0.06$ fm, due to the freezing of the topological charge.[8] Further reducing the lattice constant while retaining ergodicity of the algorithm became possible, employing open boundary conditions in the Euclidean time direction,[9] allowing so-called instantons to flow into and out of the simulated volume.
- We analyse not just the nucleon but all octet baryons, *i. e.* the nucleon (N, quark content $\ell\ell\ell$, where $\ell \in \{u, d\}$) as well as the Σ ($\ell\ell s$), the Λ ($\ell\ell s$) and the Ξ ($\ell s s$). This

is possible by employing a novel stochastic method[10–13] that was efficiently implemented by us on Xeon and Xeon-Phi platforms, employing a very general factorisation approach[14, 15] into a "spectator part" defining properties of the external baryon states and an "insertion part", corresponding to the current with which the baryon is probed.

This article is organised as follow. First we explain our simulation strategy in Sec. 2, before we show results on the quark mass dependence of octet baryon masses in Sec. 3. We then proceed to investigate flavour symmetry breaking effects on isovector charges in Sec. 4 and briefly discuss light cone distribution amplitudes in Sec. 5, before we summarise.

2 Overview of the Simulation

We employ $N_f = 2 + 1$ flavours of non-perturbatively order a improved Wilson fermions and the tree-level Symanzik improved gauge action. For details on the action and the HMC simulation, see Ref. 16. Since that publication more CLS simulation points have been added. The ensembles were generated using OPENQCD[17, 18] within the CLS[19] effort.[a] Some of this was carried out on JUWELS[21] and JUQUEEN.[22] So far six values of the inverse coupling constant $\beta = 6/g^2$ have been realised, along three quark mass plane trajectories. These cover lattice spacings $a = 0.039\,\text{fm}$ ($\beta = 3.85$) up to $a = 0.099\,\text{fm}$ ($\beta = 3.34$) and range from $\{48, 128\} \cdot 24^3$ (A, U ensembles) over $\{64, 96, 128\} \cdot 32^3$ (B, H, S), $\{96, 128\} \cdot 48^4$ (C, N), $\{128, 192\} \cdot 64^3$ (D, J) up to $192 \cdot 96^3$ (E) lattice sites. For an overview, see Fig. 1. The lattice spacing was set using $\sqrt{8t_0^*} = 0.413(6)\,\text{fm}$, with the scale t_0^* defined in Ref. 24. This value was obtained using pion and kaon decay constants. Here, we obtain a consistent but more precise value using baryon masses.

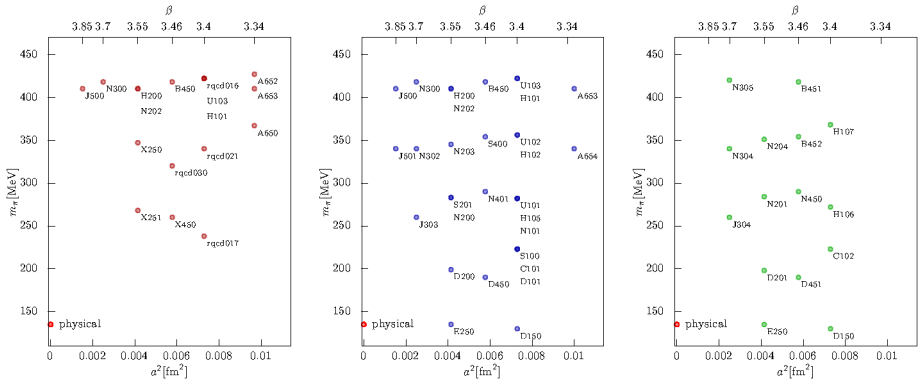

Figure 1. Analysed ensembles: the different quark mass trajectories (left: $m_s = m_\ell$, centre: $m_s + 2m_\ell = \text{const}$, right: $\widehat{m}_s \approx \text{const}$) have been analysed at six (four for $\widehat{m}_s \approx \text{const}$) different lattice spacings.

The naive scaling of the simulation cost is $\propto a^{-4}$ due to the increasing number of points if the size of the four-dimensional physical box is kept fixed. In addition autocorrelation

[a] A few additional $m_\ell = m_s$ ensembles were generated by the RQCD group employing the BQCD-Code.[20]

times will be subject to critical slowing down $\propto a^{-z}$ with $z \approx 2$, further increasing the computational effort towards the continuum limit. However, also reducing the quark mass m_ℓ does not come for free. First of all, finite size effects are suppressed exponentially with the smallest mass gap, which is the pion mass $M_\pi \propto \sqrt{m_\ell}$. If we wish to keep the lattice extent $L \gtrsim 4/M_\pi$ constant in units of the pion mass, then the volume has to be increased in proportion to M_π^{-4}. Moreover, the step size in the HMC algorithm with an Omelyan integrator scales like $L/M_\pi \propto M_\pi^{-3/2}$ while the condition number of the discretised Dirac matrix increases $\propto m_\ell^{-1} \propto M_\pi^{-2}$. The last aspect becomes less severe when employing a multigrid solver[25, 26] (see also Ref. 27) as we do for our analysis of the gauge ensembles on JURECA-Booster.[23] Due to using open boundary conditions in time,[9, 17] indeed we do not observe any severe slowing down, see Fig. 2, except for the finest lattice spacing where at present we are accruing more statistics on JUWELS. In general, autocorrelation times increase towards finer lattices, the exception being our coarsest lattice which is at the limit of what is possible to simulate with our action.

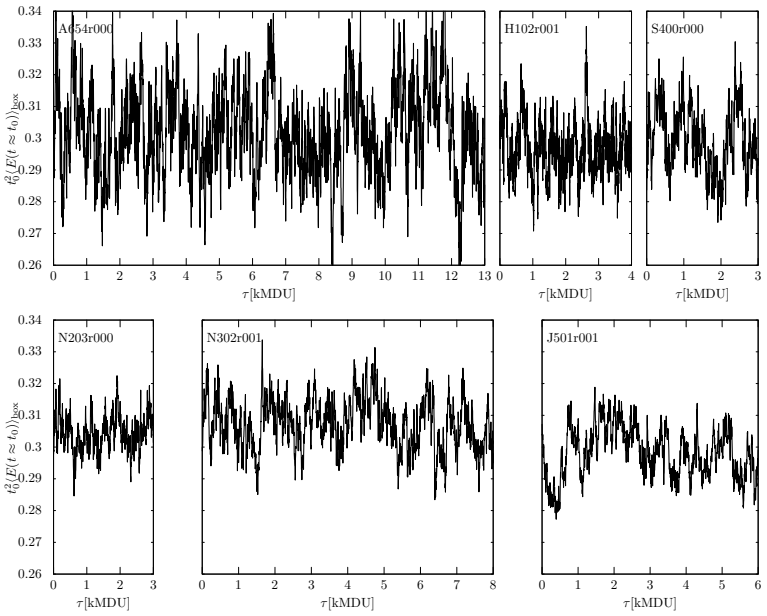

Figure 2. History of the Wilson flow action density,[28] multiplied by t_0^2,[29] after a flow time close to t_0, inside a central sub-volume of approximately 1 fm $\cdot\, (aN_s)^3$, along a line of $M_\pi \approx 340$ MeV (for $m_s + 2m_\ell = \text{const}$) from coarse to fine lattice spacings. This quantity has the largest integrated autocorrelation time. The amplitude of the fluctuation varies, *e. g.* due to somewhat different physical volumes. Autocorrelations increase from top left to bottom right, with the exception of A654 at $\beta = 3.34$ where we observe larger autocorrelation times than at $\beta = 3.4$. For the cases where more than one Monte-Carlo chain exists, only one replica is shown.

As mentioned above the ensembles are distributed along three lines in the quark mass plane: along $m_\ell = m_s$, along $2m_\ell + m_s = \text{const}$ and along a line of an approximately constant renormalised strange quark mass.[30] The simulation points for the latter two quark

mass trajectories intersect close to the physical point while the former one approaches the chiral limit $m_s = m_\ell = 0$, which is of particular interest for ChPT which is an expansion in terms of pseudoscalar meson masses about this limit. Some relations in the mesonic sector, in particular the Gell-Mann–Oakes–Renner relation, which implies the approximate proportionality $M_\pi^2 \propto m_\ell$, have been verified to surprising accuracy in lattice simulations, even at quite large pion masses. In the baryonic sector, however, BChPT often does not appear to converge very well, and for some quantities like axial charges or σ terms (*i. e.* scalar charges) it has been suggested that pion masses smaller than 200 MeV may be necessary to make contact with the regime where SU(2) BChPT is of any use.[31] This poses serious questions regarding the validity of SU(3) BChPT since the kaons and η mesons of the real world are much heavier than that. Strong interactions do not distinguish between different quark flavours and flavour symmetry is only broken by quark mass differences and by electroweak interactions, the latter being small corrections. This means that SU(3) BChPT is much more constrained than SU(2) BChPT: while the number of hadronic observables explodes, the number of independent low energy constants (LECs) increases only very moderately since $\delta m = m_s - m_\ell$ is the only flavour symmetry breaking parameter.

3 The Baryon Spectrum

In order to set the lattice scale a, to test BChPT and to determine LECs, we determine the light octet baryon spectrum. The results are shown in Fig. 3. The fit corresponds to the parametrisation

$$m_B(M_\pi, M_K, a) = m_B(M_\pi, M_K, 0)\left[1 + \bar{c}a^2\overline{M}^2 + \delta c_B a^2 \delta M^2\right] \tag{1}$$

where everything is scaled in units of the parameter $\sqrt{8t_0}$. The squared pseudoscalar mass combinations $\overline{M}^2 = (2M_K^2 + M_\pi^2)/3 \approx 2B_0\overline{m}$ and $\delta M^2 = 2M_K^2 - 2M_\pi^2 \approx 2B_0\delta m$

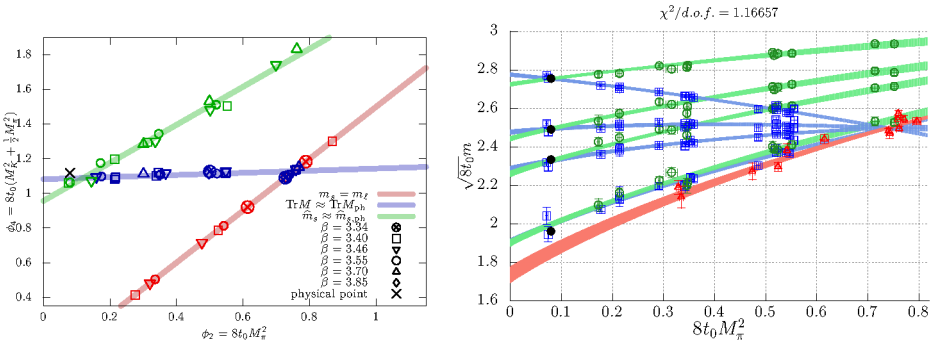

Figure 3. Left: the three lines in the quark mass plane: $m_s = m_\ell$ (red), $m_s + 2m_\ell = \text{const}$ (blue) and $\widehat{m}_s \approx \text{const}$ (green). The horizontal axis is roughly proportional to the light quark mass, the combination on the vertical axis to the sum of quark masses. Right: baryon masses as a function of the squared pion mass: Ξ, Σ, Λ, N from top to bottom. Along the $m_s = m_\ell$ trajectory (red) these are degenerated. The other two sets (blue and green) intersect at the physical pion mass. The scale t_0 was set such that the Ξ mass corresponds to the experimental value (black points).

are proportional to the average quark mass $\overline{m} = (m_s + 2m_\ell)/3$ and the flavour symmetry breaking parameter δm. There is no relation between the four δc_B so that the continuum limit behaviour is encapsulated into six parameters. The quark mass dependence of the continuum limit baryon masses shown in the figure corresponds to NNLO, *i. e.* $\mathcal{O}(p^3)$ BChPT[32] in the EOMS scheme.[33] To this order four parameters are needed to describe this dependence so that in total the combined fit only contains ten parameters. The data points shown are shifted along the fit to $a = 0$ and interpolated to the strange quark masses that exactly correspond to the trajectories. We also carried out a multitude of other fits, with similar results. We find $\sqrt{8t_{0,\mathrm{ph}}} = 0.4128(22)$ MeV, with a systematic error that still needs to be determined. From these fits one can also infer the σ term $\sigma_{\pi N} = 41(2)$ fm, where again the error given is purely statistical for the moment being. Nevertheless, it is clear by now that the total error will be very competitive. The number agrees with earlier lattice QCD determinations[4–7] but disagrees with current phenomenological estimates.[2, 3]

Clearly, the data are in agreement with experiment and well described by the fit. It still needs to be studied to what extent the LECs are universal, *i. e.* if this agreement with the BChPT parametrisation is accidental and higher order terms need to be included. Two LECs appear at order p^2, which corresponds to a linear fit. The curvature is due to the remaining two LECs F and D that appear at $\mathcal{O}(p^3)$ in SU(3) BChPT. These are related to axial charges of octet baryons, for instance the axial charge of the nucleon in the chiral limit reads $\mathring{g}_A = F + D$.

4 Baryon Isovector Charges

Isovector charges are defined as matrix elements of local operators at zero momentum transfer. Here we consider two kinds of (generalised) charges:

$$g_J^B = \langle B|O(\Gamma_J)|B\rangle, \quad J \in \{V, A, T, S\} \tag{2}$$

$$m_B\langle x\rangle_J^B = \langle B|O(\Gamma_J)|B\rangle, \quad J \in \{u^+ - d^+, \Delta u^- - \Delta d^-, \delta u^+ - \delta d^+\} \tag{3}$$

where $q^\pm = q \pm \bar{q}$. The Γ-structures of the latter currents that correspond to the second Mellin moment of parton distribution functions contain one derivative and in both cases we use isovector combinations $O(\Gamma_J) = \bar{u}\Gamma_J u - \bar{d}\Gamma_J d$, for details see Ref. 15.

Assuming SU(3) flavour symmetry, the axial vector charges can be expressed as combinations of just two variables:

$$g_A^N = F + D, \qquad g_A^\Sigma = 2F, \qquad g_A^\Xi = F - D \tag{4}$$

In the chiral limit these correspond to the LECs discussed above. We can directly extract these LECs, extrapolating the combinations $F = (g_A^N + g_A^\Xi)/2$ and $D = (g_A^N - g_A^\Xi)/2$ along the $m_\ell = m_s$ trajectory as illustrated in Fig. 4. This is the only lattice determination so far of these LECs in the SU(3) chiral limit. We ultimately aim at carrying out a combined BChPT fit both to the spectrum and the charges in the continuum limit.

In the case of flavour symmetry, *i. e.* $m_s = m_\ell$, also all the other octet charges g_J can each be parameterised in terms of two parameters F_J and D_J. According to Eq. 4, in this limit $(g_J^N + g_J^\Xi)/g_J^\Sigma = (2F_J)/(2F_J) = 1$ holds. Consequently, We can quantify the SU(3) breaking effect in terms of the parameter

$$\delta_{\mathrm{SU(3)}}^J = \left(g_J^N + g_J^\Xi\right)/g_J^\Sigma - 1 \tag{5}$$

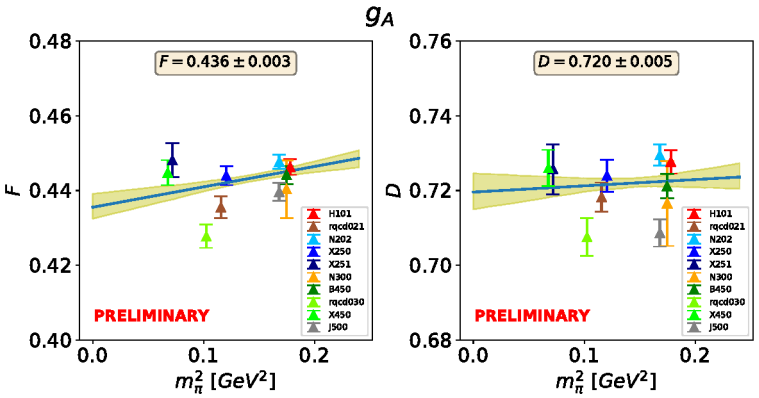

Figure 4. The parameters F and D, extrapolated along the $m_s = m_\ell$ line to the chiral limit. Lattice spacing and finite volume effects are not as yet resolved and the data shown are raw data that have not been shifted to the continuum, infinite volume limit.

It turns out that while these symmetry breaking effects amount to about 10 % at the physical quark mass point for $g_A = \langle \mathbb{1} \rangle_{\Delta u^+ - \Delta d^+}$ and $\langle x \rangle_{\Delta u^- - \Delta d^-}$, these appear to be negligible for g_T and $\langle x \rangle_{u^+ - d^+}$.[15] At present we are carrying out chiral and continuum limit extrapolations similar to those shown for the masses above.

5 Baryon Distribution Amplitudes

Within the parton model description of deep inelastic scattering PDFs can be viewed as probability densities of a particular quark or gluon to carry a fraction x of the longitudinal momentum of the baryon. Radiative QCD corrections and higher twist contributions complicate this simplistic picture. Moments of PDFs, namely the generalised charges introduced above, can be expressed in terms of matrix elements involving local operators which can be computed in Euclidean spacetime using Lattice QCD. PDFs are important in the description of inclusive processes. In contrast, light cone distribution amplitudes (DAs) correspond to probability wavefunctions, where transverse momenta are integrated out. These are needed for the description of exclusive processes and are much harder to constrain experimentally than PDFs. Interestingly, in this case at leading twist the longitudinal momentum fractions of the valence quarks q_1, q_2 and q_3 sum up to 1 ($x_1 + x_2 + x_3 = 1$), *i. e.* effects of the gluons and sea quarks are suppressed by powers of the inverse momentum transfer. Moreover, in this case at large scales an asymptotic shape is approached (in the baryon case $120 x_1 x_2 x_3$). Deviations from this form can be parameterised in terms of the first few moments since higher moments are suppressed due to their larger anomalous dimensions, for details, see Refs. 34, 35. This is quite different from the PDF situation. It turns out that lattice spacing effects are very significant for baryon DAs and, for the first time, we have determined their normalisations and first moments in the continuum limit.[35] The normalisations f^B also play a role in hypothetical proton decay involving operators that convert two quarks into an antiquark. We have reconstructed the three leading twist

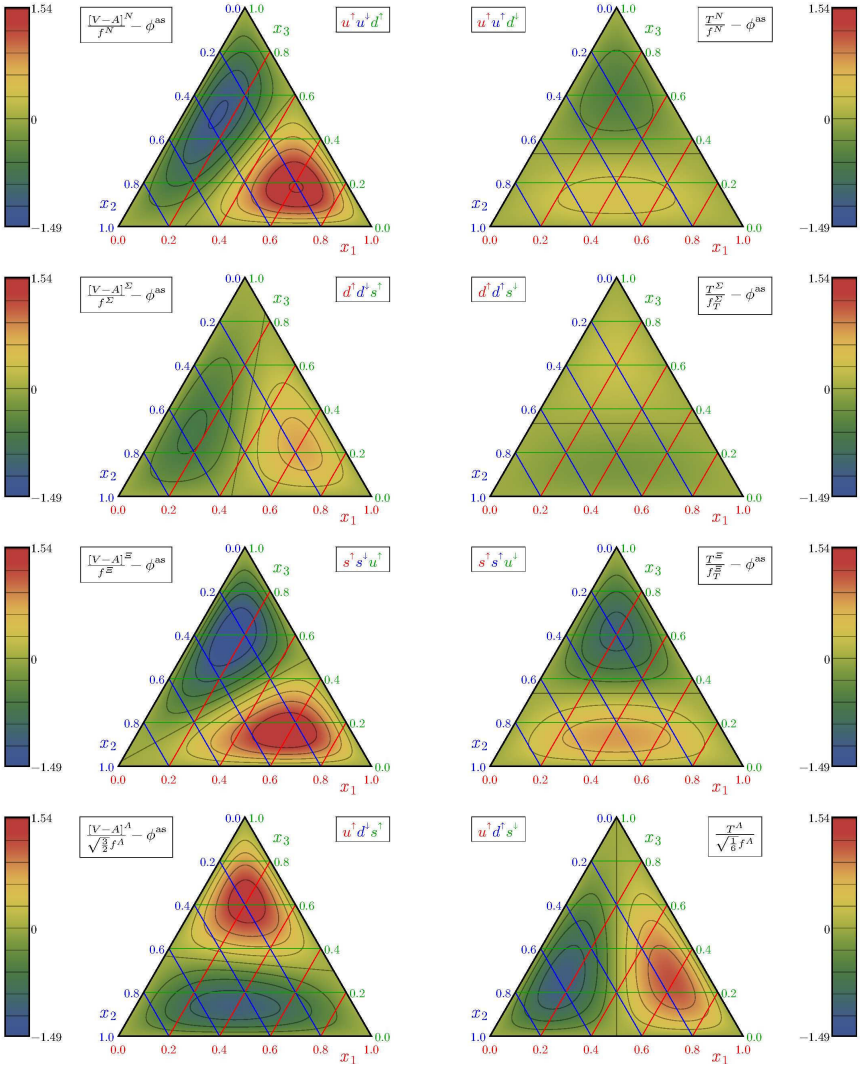

Figure 5. Barycentric figures ($x_1 + x_2 + x_3 = 1$) showing the deviation of the DAs $[V-A]^B$ (left) and T^B (right) from the respective asymptotic limits $120 x_1 x_2 x_3$ and 0, respectively.[35]

DAs V^B, A^B and T^B using the first moments in x_i at a scale $\mu = 2\,\text{GeV}$. Of particular interest are deviations from the (symmetric) asymptotic shape. These are plotted in Fig. 5, where the combinations $V^B - A^B$ and T^B are accompanied by definite helicities of the quarks involved. Within the proton (first row) the "leading" u quark with its helicity aligned to that of the proton carries a larger momentum fraction: $x_1 > x_2 \approx x_3$. This is the only lattice determination of these quantities in the continuum limit.

6 Summary

We were able to obtain for the first time controlled continuum limit results for various baryonic observables. Here we highlighted just a few results of an extensive simulation programme and we did not even comment on the non-perturbative renormalisation and order a improvement that was carried out as well or other technical details.

Acknowledgements

The work of GB is funded by BMBF grant 05P18WRFP1. Support was also provided by the DFG SFB/TRR 55 and the EU ITN EuroPLEx (grant 813942). We thank all our collaborators in RQCD and CLS. We gratefully acknowledge computing time granted by the John von Neumann Institute for Computing (NIC), provided on the Booster partition of the supercomputer JURECA[23] at Jülich Supercomputing Centre. Additional simulations were carried out at the QPACE 3 Xeon Phi cluster of SFB/TRR 55.

References

1. A. Loureiro *et al.*, *On the upper bound of neutrino masses from combined cosmological observations and particle physics experiments*, Phys. Rev. Lett. **123**, 081301, 2019.
2. M. Hoferichter, J. Ruiz de Elvira, B. Kubis, and U. G. Meißner, *High-precision determination of the pion-nucleon σ term from Roy-Steiner equations*, Phys. Rev. Lett. **115**, 092301, 2015.
3. J. Ruiz de Elvira, M. Hoferichter, B. Kubis, and U. G. Meißner, *Extracting the σ-term from low-energy pion-nucleon scattering*, J. Phys. G **45**, 024001, 2018.
4. S. Dürr *et al.*, *Lattice computation of the nucleon scalar quark contents at the physical point*, Phys. Rev. Lett. **116**, 172001, 2016.
5. Y. B. Yang *et al.* [χQCD Collaboration], *πN and strangeness sigma terms at the physical point with chiral fermions*, Phys. Rev. D **94**, 054503, 2016.
6. A. Abdel-Rehim *et al.* [ETM Collaboration], *Direct evaluation of the quark content of nucleons from Lattice QCD at the physical point*, Phys. Rev. Lett. **116**, 252001, 2016.
7. G. S. Bali *et al.* [RQCD Collaboration], *Direct determinations of the nucleon and pion σ terms at nearly physical quark masses*, Phys. Rev. D **93**, 094504, 2016.
8. S. Schaefer *et al.* [ALPHA Collaboration], *Critical slowing down and error analysis in Lattice QCD simulations*, Nucl. Phys. B **845**, 93–119, 2011.
9. M. Lüscher and S. Schaefer, *Lattice QCD without topology barriers*, JHEP **1107**, 036, 2011.
10. R. Evans, G. Bali, and S. Collins, *Improved semileptonic form factor calculations in Lattice QCD*, Phys. Rev. D **82**, 094501, 2010.
11. C. Alexandrou *et al.* [ETM Collaboration], *A stochastic method for computing hadronic matrix elements*, Eur. Phys. J. C **74**, 2692, 2014.
12. G. S. Bali *et al.*, *Nucleon structure from stochastic estimators*, PoS LAT **2013**, 271, 2014.

13. Y. B. Yang, A. Alexandru, T. Draper, M. Gong, and K. F. Liu, *Stochastic method with low mode substitution for nucleon isovector matrix elements*, Phys. Rev. D **93**, 034503, 2016.
14. G. S. Bali *et al.*, *Baryonic and mesonic 3-point functions with open spin indices*, EPJ Web Conf. **175**, 06014, 2018.
15. G. S. Bali *et al.*, *Hyperon couplings from $N_f = 2 + 1$ Lattice QCD*, PoS LAT **2019**, 099, 2019.
16. M. Bruno *et al.*, *Simulation of QCD with $N_f = 2 + 1$ flavors of non-perturbatively improved Wilson fermions*, JHEP **1502**, 043, 2015.
17. M. Lüscher and S. Schaefer, *Lattice QCD with open boundary conditions and twisted-mass reweighting*, Comput. Phys. Commun. **184**, 519, 2013.
18. `http://luscher.web.cern.ch/luscher/openQCD/`
19. `https://wiki-zeuthen.desy.de/CLS/`
20. Y. Nakamura and H. Stüben, *BQCD – Berlin quantum chromodynamics program*, PoS LAT **2010**, 040, 2010.
21. D. Krause, *JUWELS: Modular Tier-0/1 Supercomputer at the Jülich Supercomputing Centre*, JLSRF **5**, A135, 2019.
22. M. Stephan and J. Docter, *JUQUEEN: IBM Blue Gene/Q Supercomputer System at the Jülich Supercomputing Centre*, JLSRF **1**, A1, 2015.
23. D. Krause and P. Thörnig, *JURECA: Modular supercomputer at Jülich Supercomputing Centre*, JLSRF **4**, A132, 2018.
24. M. Bruno, T. Korzec, and S. Schaefer, *Setting the scale for the CLS $2 + 1$ flavor ensembles*, Phys. Rev. D **95**, 074504, 2017.
25. S. Heybrock, M. Rottmann, P. Georg, and T. Wettig, *Adaptive algebraic multigrid on SIMD architectures*, PoS LAT **2015**, 036, 2016.
26. P. Georg, D. Richtmann, and T. Wettig, *DD-αAMG on QPACE 3*, EPJ Web Conf. **175**, 02007, 2018.
27. A. Frommer, K. Kahl, S. Krieg, B. Leder, and M. Rottmann, *Adaptive aggregation based domain decomposition multigrid for the lattice Wilson Dirac operator*, SIAM J. Sci. Comput. **36**, A1581–A1608, 2014.
28. M. Lüscher, *Trivializing maps, the Wilson flow and the HMC algorithm*, Commun. Math. Phys. **293**, 899–919, 2010.
29. M. Lüscher, *Properties and uses of the Wilson flow in Lattice QCD*, JHEP **1008**, 071, 2010, [Erratum: JHEP **1403**, 092, 2014].
30. G. S. Bali *et al.* [RQCD Collaboration], *Lattice simulations with $N_f = 2+1$ improved Wilson fermions at a fixed strange quark mass*, Phys. Rev. D **94**, 074501, 2016.
31. G. S. Bali *et al.*, *Nucleon isovector couplings from $N_f = 2$ Lattice QCD*, Phys. Rev. D **91**, 054501, 2015.
32. P. J. Ellis and K. Torikoshi, *Baryon masses in chiral perturbation theory with infrared regularization*, Phys. Rev. C **61**, 015205, 2000.
33. J. Gegelia and G. Japaridze, *Matching heavy particle approach to relativistic theory*, Phys. Rev. D **60**, 114038, 1999.
34. G. S. Bali *et al.*, *Light-cone distribution amplitudes of the baryon octet*, JHEP **1602**, 070, 2016.
35. G. S. Bali *et al.* [RQCD Collaboration], *Light-cone distribution amplitudes of octet baryons from lattice QCD*, Eur. Phys. J. A **55**, 116, 2019.